Superconducting order parameter of Sr_2RuO_4: a microscopic perspective

Aline Ramires[1, 2, 3] and Manfred Sigrist[4]

[1]*Max Planck Institute for the Physics of Complex Systems, Dresden, 01187, Germany*
[2]*ICTP-SAIFR, International Centre for Theoretical Physics - South American*
Institute for Fundamental Research, São Paulo, SP, 01140-070, Brazil
[3]*Instituto de Física Teórica - Universidade Estadual Paulista, São Paulo, SP, 01140-070, Brazil*
[4]*Institute for Theoretical Physics, ETH Zurich, CH-8093, Zurich, Switzerland*
(Dated: September 5, 2019)

The character of the superconducting phase of Sr_2RuO_4 is topic of a longstanding discussion. The classification of the symmetry allowed order parameters has relied on the tetragonal symmetry of the lattice and on cylindrical Fermi surfaces, usually taken to be featureless, not including the non-trivial symmetry aspects related to their orbital content. Here we show how the careful account of the orbital degree of freedom and a three dimensional description lead to a much richer classification of order parameters. We analyse the stability and degeneracy of these new order parameters from the perspective of the concept of *superconducting fitness* and propose new order parameter candidates which can systematically account for the observed phenomenology in this material.

I. INTRODUCTION

Sr_2RuO_4 is among the materials with the highest quality single-crystals[1,2] and with the best characterized normal state Fermi surfaces[3–6]. Yet, the nature of the superconducting state in this material remains controversial for more than 20 years[7]. Experimental evidence from different probes give us conflicting information if we try to understand the phenomenology of this material from the perspective of an order parameter on a single cylindrical Fermi surface. The solution to this conundrum might rely on the fact that Sr_2RuO_4 is a complex material, since the faithful description of its normal state electronic structure requires at least the three Ru 4d orbitals in the t_{2g} manifold. In contrast to the microscopic description in the orbital basis, superconductivity is usually understood as an instability out of a Fermi surface. When studying superconductivity in Sr_2RuO_4 it is usual to erase the microscopic complexity needed for the realistic representation of its three Fermi surfaces, and to start treating these as featureless entities[8–11].

Several experiments have indicated that the order parameter is in the spin-triplet sector, in particular Knight shift[12,13] and neutron scattering measurements[14], which observed no change in the spin susceptibility across the superconducting critical temperature, T_c, for any magnetic field direction. Another important piece of evidence is the observation of the onset of time-reversal symmetry breaking (TRSB) at T_c from muon spin rotation[15,16] and polar Kerr effect measurements[17]. These two facts together point towards a chiral order parameter with a d-vector $\mathbf{d}(\mathbf{k}) = (0, 0, k_x \pm ik_y)$[1,18–20], the only unitary odd-parity triplet order parameter in a tetragonal material to break time-reversal symmetry. Contradictions emerge once we consider complementary experimental results. For example, specific heat[21–25] and ultrasound[26] measurements suggest the presence of horizontal line nodes in the superconducting gap, and new thermal conductivity measurements[27] give evidence for vertical line nodes. In addition, recent experiments are now chal-

lenging what were thought to be well stablished results. In particular, novel Knight shift measurements indicate a drop in the spin susceptibility for in-plane magnetic fields, challenging the proposal of an order parameter with a d-vector along the z-direction[28]. Also, latest uniaxial strain experiments performed at the micron-scale observe no obvious splitting of the critical temperature as a function of strain, expected if the order parameter has two-components[29]. These recent results motivate us to look more carefully into the possible order parameters for Sr_2RuO_4 from a microscopic perspective.

This paper is organized as follows: In Section II we introduce the most general model for the normal state of Sr_2RuO_4 based on the presence of time-reversal symmetry, the point group symmetry D_{4h} (which includes inversion symmetry) and the nature of the underlying orbital degrees of freedom (DOF) in the t_{2g} manifold. In Section III we reclassify the order parameters, considering explicitly the orbital dependence, discuss their properties and probe these against the most recent experimental results. In Section IV we focus on intra-orbital order parameters and apply the concept of *superconducting fitness*, which allows for a qualitatively understanding of the stability of each order parameter. From this analysis, we also discuss the presence of symmetry protected and accidental or quasi-degeneracies and the consequences for experiments under strain. We conclude with Section V, summarizing our results and highlighting new directions for theoretical investigation for a more complete understanding of Sr_2RuO_4.

II. THE NORMAL STATE HAMILTONIAN

Sr_2RuO_4 has the tetragonal space group $I4/mmm$, or #139[1]. This group consists of operations in the point group D_{4h} and intra-unit-cell shifts by half a lattice parameter in all directions. Focusing on the point group, here we refer to D_4 since in this case the tables below have a more compact form (the product with inversion

essentially splits the representations in even and odd). It is well known that the important DOF for the description of Sr_2RuO_4 are the electrons in the t_{2g} orbital manifold in the Ru ions, namely d_{yz}, d_{xz} and d_{xy}. Choosing the basis $\Phi_{\mathbf{k}}^\dagger = (c_{yz\uparrow}^\dagger, c_{yz\downarrow}^\dagger, c_{xz\uparrow}^\dagger, c_{xz\downarrow}^\dagger, c_{xy\uparrow}^\dagger, c_{xy\downarrow}^\dagger)_{\mathbf{k}}$, one can construct the most general three-orbital single-particle Hamiltonian describing the normal state as:

$$\mathcal{H}_0(\mathbf{k}) = \Phi_{\mathbf{k}}^\dagger H_0(\mathbf{k})\Phi_{\mathbf{k}}, \qquad (1)$$

with

$$H_0(\mathbf{k}) = \sum_{a,b} h_{ab}(\mathbf{k})[\lambda_a \otimes \sigma_b], \qquad (2)$$

where $h_{ab}(\mathbf{k})$ are 36 real functions of momenta $\mathbf{k}$, $\lambda_{a=1,\dots,8}$ are the Gell-Mann matrices and $\lambda_0 = \sqrt{\frac{2}{3}}I_3$, with I_3 the three-dimensional identity matrix, standing for the orbital DOF, and $\sigma_{b=1,2,3}$ are Pauli matrices, with σ_0 the two-dimensional identity matrix, standing for the spin DOF. The explicit form of the Gell-Mann and Pauli matrices used in this work are given in Appendix A.

Requiring the Hamiltonian to be invariant under inversion and time-reversal, we find restrictions on the allowed pairs of indices (a,b). Inversion, $P = \sqrt{\frac{3}{2}}\lambda_0 \otimes \sigma_0$, acts trivially on the spin and orbital DOF:

$$PH_0(\mathbf{k})P^{-1} = H_0(\mathbf{k}) \qquad (3)$$

implying that the functions $h_{ab}(\mathbf{k}) = h_{ab}(-\mathbf{k})$ must all be even in momentum. Time-reversal, $\Theta = K\sqrt{\frac{3}{2}}\lambda_0 \otimes (i\sigma_2)$, with K standing for complex conjugation, acts on the spin DOF:

$$\Theta H_0(\mathbf{k})\Theta^{-1} = H_0(\mathbf{k}), \qquad (4)$$

implying $h_{ab}(\mathbf{k}) = \pm h_{ab}^*(-\mathbf{k})$, with the plus (minus) sign for imaginary (real) products $[\lambda_a \otimes \sigma_b]$. The explicit pairs of indices (a,b) are summarized in Table I. Given that the functions $h_{ab}(\mathbf{k})$ are real and must be even in $\mathbf{k}$, only a subset of 15 pairs (a,b) is in fact allowed in the Hamiltonian.

The Hamiltonian should also be invariant under the point group operations associated with D_4. Selecting as generators C_4 (rotation along the z-axis by $\pi/2$), C_2' (rotation along the x-axis by π) and C_2'' (rotation along the diagonal $x = y$ by π), the basis matrices $[\lambda_a \otimes \sigma_b]$ transform as specific irreducible representations of the point group. The invariance of the Hamiltonian $H_0(\mathbf{k})$ under the point group requires that the basis functions $h_{ab}(\mathbf{k})$ transform under the same irreducible representation as the associated basis matrices. The explicit form of the point group operators are given in Appendix B, and the result of the symmetry analysis for the normal state Hamiltonian is summarized in Table II.

Note that the form we find through this symmetry analysis is in accordance with the well stablished Hamiltonian for Sr_2RuO_4[30,31], in which the terms $(0,0)$, $(7,0)$ and $(8,0)$ are associated with intra-orbital hopping in

$h_{ab}(\mathbf{k})$	(a,b)	N
Even	$(\{0,1,2,3,7,8\},2)$ and $(\{4,5,6\},\{0,1,3\})$	15
Odd	$(\{4,5,6\},2)$ and $(\{0,1,2,3,7,8\},\{0,1,3\})$	21

TABLE I. Parity of $h_{ab}(\mathbf{k})$ functions according to time-reversal symmetry. N indicates the number of pairs (a,b) for each parity.

Irrep	(a,b)	Type	Only in 3D
A_1	$(0,0)$	intra-orbital hopping	
	$(8,0)$	intra-orbital hopping	
	$(4,3)$	atomic SOC	
	$(5,2)-(6,1)$	atomic-SOC	
A_2	$(5,1)+(6,2)$	**k**-SOC	✓
B_1	$(7,0)$	intra-orbital hopping	
	$(5,2)+(6,1)$	**k**-SOC	✓
B_2	$(1,0)$	inter-orbital hopping	
	$(5,1)-(6,2)$	**k**-SOC	✓
$E(i)$	$(3,0)$	inter-orbital hopping	✓
	$-(2,0)$	inter-orbital hopping	✓
$E(ii)$	$(4,2)$	**k**-SOC	✓
	$-(4,1)$	**k**-SOC	✓
$E(iii)$	$(5,3)$	**k**-SOC	✓
	$(6,3)$	**k**-SOC	✓

TABLE II. List of the 15 symmetry allowed terms in the normal state Hamiltonian $H_0(\mathbf{k})$ given by Eq.2. For each (a,b), the basis function $h_{ab}(\mathbf{k})$ should transform according to a specific irreducible representation (Irrep), and can be associated with different physical processes (Type). Here **k**-SOC stands for even-momentum spin-orbit coupling. The last column highlights which symmetry allowed terms are present only in three-dimensional models. For the two-dimensional Irreps $E(\alpha)$, $\alpha = i, ii, iii$, the entries are organized such that the first (a,b) term transforms as x and the second as y.

the A_1, B_1 and A_1 representations, respectively; $(1,0)$ is associated with inter-orbital hopping in B_2, allowed only between xz and yz orbitals; and $(4,3)$ and $(5,2)-(6,1)$ in A_1 are associated with atomic spin-orbit coupling (SOC). Other allowed terms are: $\{(3,0),(-2,0)\}$ in E, related to out-of-plane inter-orbital hopping between xz or yz and xy orbitals; $\{(4,2),-(4,1)\}$ and $\{(5,3),(6,3)\}$ also in E, as well $(5,2)+(6,1)$ and $(5,1)\pm(6,2)$ in B_1, A_2 and B_2, respectively, all related to even k-dependent SOC, which are usually not taken into account within two-dimensional models.

III. THE ORDER PARAMETERS IN THE ORBITAL BASIS

In multiorbital superconducting systems, the effective Bogoliubov-de Gennes Hamiltonian can be written as:

$$H_{BdG} = \sum_{\mathbf{k}} \Psi_{\mathbf{k}}^{\dagger} \begin{pmatrix} H_0(\mathbf{k}) & \Delta(\mathbf{k}) \\ \Delta^{\dagger}(\mathbf{k}) & -H_0^*(-\mathbf{k}) \end{pmatrix} \Psi_{\mathbf{k}}, \qquad (5)$$

in terms of the *multi-orbital Nambu spinors*:

$$\Psi_{\mathbf{k}}^{\dagger} = (\Phi_{\mathbf{k}}^{\dagger}, \Phi_{-\mathbf{k}}^{T}), \qquad (6)$$

with $\Phi_{\mathbf{k}}^{\dagger}$ and $H_0(\mathbf{k})$ defined above for the case of Sr_2RuO_4. Here $\Delta(\mathbf{k})$ is the gap matrix which can describe both spin singlet and triplet pairing in multi-orbital space.

Similarly to the parametrization of the normal state Hamiltonian, we start parametrizing the gap matrix with 36 functions $d_{ab}(\mathbf{k})$:

$$\Delta(\mathbf{k}) = \sum_{a,b} d_{ab}(\mathbf{k})[\lambda_a \otimes \sigma_b(i\sigma_2)]. \qquad (7)$$

In analogy to the *d-vector* parametrizing the triplet order parameter for a single band superconductor, here we introduce a *d-tensor* notation, $d_{ab}(\mathbf{k})$. In order to satisfy the anti-symmetry of the pair wave-function, the order parameter should follow

$$\Delta(\mathbf{k}) = -\Delta^T(-\mathbf{k}), \qquad (8)$$

such that we can separate the functions $d_{ab}(\mathbf{k})$ in even- or odd-parity if the tensor product $[\lambda_a \otimes \sigma_b(i\sigma_2)]$ is anti-symmetric or symmetric, respectively. Interestingly the pairs of $[a,b]$ associated with even or odd $d_{ab}(\mathbf{k})$ functions are the same as the ones identified for the normal state Hamiltonian parameters $h_{ab}(\mathbf{k})$ summarized in Table I. This can be understood by the fact that the basis matrices chosen here are all Hermitian, such that the transpose is equivalent to the complex conjugate, making the correspondence to time-reversal symmetry. Note that, in order to distinguish the parametrization of the gap matrix from the parametrization of the normal state Hamiltonian, we use different brakets $[a,b]$ for the gap function indexes.

We can further classify the order parameters considering the point group transformations, which rotate the order parameter as $U\Delta(\mathbf{k})(U^{-1})^{*31,32}$. We start the analysis looking at how the product $[\lambda_a \otimes \sigma_b(i\sigma_2)]$ transforms under the generators of the point group, what allows us to associate these matrices with distinct irreducible representations (Irreps) of D_4. The properties of all basis matrices are listed in detail in Appendix C. Here we focus on intra-orbital pairing, $a = \{0,7,8\}$, and summarize the properties of the basis matrices in the first four columns of Table III .

We can now introduce the non-trivial momentum dependence of $d_{ab}(\mathbf{k})$ (see form factors in Fig. 1). In order

$[a,b]$	Irrep	Spin	$d_{ab}(\mathbf{k})$	A_1	A_2	B_1	B_2	E
$[0,0]$ or $[8,0]$	A_1	S	Even	A_1	A_2	B_1	B_2	E
$[7,0]$	B_1	S	Even	B_1	B_2	A_1	A_2	E
$[0,3]$ or $[8,3]$	A_2	T	Odd	A_2	A_1	B_2	B_1	E
$[7,3]$	B_2	T	Odd	B_2	B_1	A_2	A_1	E
$\{[a,1],[a,2]\}$	E	T	Odd	E	E	E	E	A_1, A_2, B_1, B_2

TABLE III. Symmetry of the order parameter with matrix basis $[\lambda_a \otimes \sigma_b(i\sigma_2)]$, represented by $[a,b]$ (first column) and function $d_{ab}(\mathbf{k})$ in different Irreps (first line of last five columns), for intra-orbital pairing $a = \{0,7,8\}$. The second column gives the representation of the matrix basis, the third column the spin character singlet (S) or triplet (T), and the fourth column the parity of the function $d_{ab}(\mathbf{k})$.

to determine the Irrep of the complete order parameter, we need to take the product of the Irrep of $d_{ab}(\mathbf{k})$ with the Irrep of $[\lambda_a \otimes \sigma_b(i\sigma_2)]$. The resulting Irrep can be inferred from the character table of the point group (see Appendix B), and the results are summarized in the last five columns of Table III for the intra-orbital components of the order parameter.

A. Properties of the order parameters

We now go over Table III, analysing in detail the symmetry properties of the order parameters in different sectors (indicated by different colors), and summarize the key experimental signatures in Table IV. In the next section we discuss which of these sectors consistently account for the features observed in the most recent experiments.

The order parameters in the yellow sector (i) are spin singlets, have even $d_{ab}(\mathbf{k}) \sim$ cte, do not carry symmetry protected nodes, and are associated with one-dimensional representations. The superconducting states in the orange sector (ii) are also spin singlets, but now $d_{ab}(\mathbf{k}) \sim k_x k_y(k_x^2 - k_y^2)$, $(k_x^2 - k_y^2)$ or $k_x k_y$ for even functions in the A_2, B_1 or B_2 representations (according to the first line of Table III). All these order parameters are associated with symmetry protected vertical line nodes and once we take the product of the representations of the matrix part $[\lambda_a \otimes \sigma_b(i\sigma_2)]$ with the function $d_{ab}(\mathbf{k})$, we find order parameters belonging to one of the one-dimensional representations A_1, A_2, B_1 or B_2. The order parameters in the red sector (iii) are also singlets, but now the even basis functions $d_{ab}(\mathbf{k}) \sim \{k_x k_z, k_y k_z\}$ belong to a two-dimensional representation. Note that now we are guaranteed to have at least horizontal line nodes (assuming that a chiral state would be energetically more favourable, in which the two
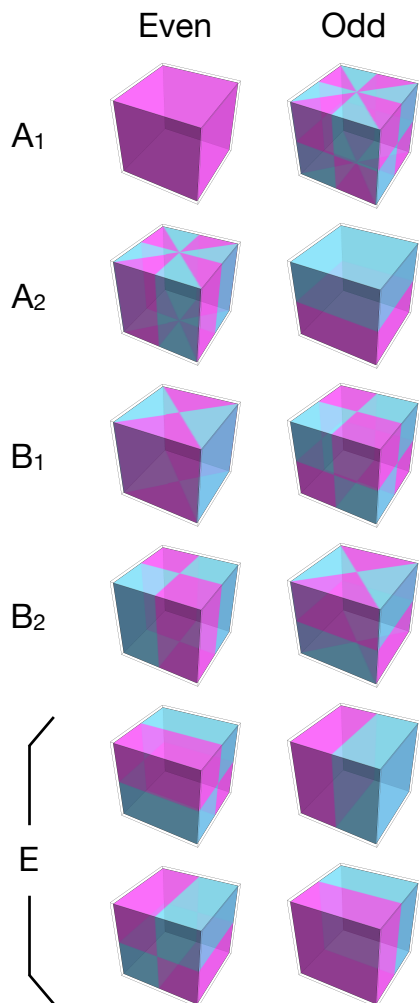
FIG. 1. Form factors associated with the (lowest power) even and odd basis functions of each of the irreducible representations of the D_4 point group. The different colors indicate positive and negative values.

	Spin	Nodes	2D-Rep
i	S	$\times$	$\times$
ii	S	v	$\times$
iii	S	h	$\checkmark$
iv	$T(z)$	hv	$\times$
v	$T(z)$	h or hv	$\times$
vi	$T(z)$	$\times$	$\checkmark$
vii	$T(p)$	hv	$\checkmark$
viii	$T(p)$	h or hv	$\checkmark$
ix	$T(p)$	$\times$	$\times$

TABLE IV. Summary of the key experimental signatures for the different families of superconducting order parameters listed in Table III. (i-ix) can be identified by the color scheme or by reading the sectors highlighted by thick lines from left to right, top to bottom in Table III. Here S stands for singlet and T for triplet (z and p correspond to the d-vector direction along the z-axis or in plane), h stands for horizontal, v for vertical and hv for simultaneous h and v line nodes.

$d_{ab}(\mathbf{k}) \sim k_x k_y k_z (k_x^2 - k_y^2)$ encodes both horizontal and vertical line nodes, and the order parameters fall in the one-dimensional representations A_2 or B_2. In the blue sector (v) we also find triplet states with a d-vector along the z-direction, but now the odd form factor $d_{ab}(\mathbf{k}) \sim k_z$, $k_z k_x k_y$ or $k_z(k_x^2 - k_y^2)$ in the A_2, B_1 or B_2 representations, respectively, with only horizontal or both horizontal and vertical symmetry protected line nodes. The order parameters in this sector fall in one of the one-dimensional representations A_1, A_2, B_1 or B_2. The dark blue sector (vi) includes triplet order parameters with a d-vector along the z-direction, and come with odd basis functions $d_{ab}(\mathbf{k}) \sim \{k_x, k_y\}$ associated with the two-dimensional representation E. For this sector the presence of nodes is not guaranteed since a chiral state is expected to be energetically more favourable, and the complete order parameter belongs to the two-dimensional representation E.

The last row in Table III includes triplet order parameters with a d-vector in plane. For this configuration, a magnetic field along the z-direction does not cause paramagnetic limiting, while an in-plane field breaks the pairs. Note also that now the matrix part of the order parameter forms itself a two-dimensional representation, denoted by $\{[a, 1], [a, 2]\}$ in the table, indicating that the matrices $[a, 1]$ and $[a, 2]$ transform as basis of the two-dimensional representation E under the point group operations. In the light green sector (vii) these basis matrixes are combined with an odd form factor $d_{ab}(\mathbf{k}) \sim k_x k_y k_z (k_x^2 - k_y^2)$ encoding both horizontal and vertical line nodes. The product of the matrix com-

components appear in a complex superposition eliminating the vertical line nodes). The fact that the matrix part $[\lambda_a \otimes \sigma_b(i\sigma_2)]$ are associated with one-dimensional representations and the function $d_{ab}(\mathbf{k})$ is associated with the two-dimensional representation, makes the complete order parameters transform as the two-dimensional representation E.

Moving on now to the triplet states, these are usually parametrized in terms of a d-vector, which gives the direction perpendicular to the orientation of the Cooper pair spin. Here the direction of the d-vector in the standard notation is encoded in the label b in $[a, b]$, as can be inferred from the matrix form $[\lambda_a \otimes \sigma_b(i\sigma_2)]$. In the cyan sector ($iv$) we find triplet states with the d-vector along the z-direction, corresponding to in-plane equal spin pairing. In this configuration, an in-plane magnetic field does not lead to paramagnetic depairing, in contrast to a field along the z-axis. In this sector, the odd function

ponent of the order parameters belonging to the two-dimensional representation E with a form factor $d_{ab}(\mathbf{k})$ in a one-dimensional representation leads to an order parameter belonging to the two-dimensional representation E. The order parameters in the green sector ($viii$) are also triplet states with an in-plane d-vector, but now the odd form factors $d_{ab}(\mathbf{k}) \sim k_z$, $k_z k_x k_y$ or $k_z(k_x^2 - k_y^2)$ in the A_2, B_1 or B_2 representations, respectively, have only horizontal or both horizontal and vertical symmetry protected line nodes. Given the product of the representations of the matrix and the form factor components of the order parameters, the complete states in this sector transform within the two-dimensional representation E. Finally, the order parameters in the dark green sector (ix) are also triplet states with an in-plane d-vector, now with odd basis functions $d_{ab}(\mathbf{k}) \sim \{k_x, k_y\}$ associated with the two dimensional representation E. Given that now both the matrix content and the form factors belong to the two-dimensional representation E, we need to consider the product $E \times E$ to define the Irrep of the complete order parameter. This product is decomposed in the one-dimensional Irreps A_1, A_2, B_1 or B_2, as indicated in Table III. Note that, in analogy to the helical states in the original classification, these states are also fully gapped.

B. Connection with recent experiments

The most recent Knight shift measurements indicate that there is a substantial drop in the spin susceptibility across the superconducting transition for in-plane magnetic fields[28]. This observation is not easy to reconcile with a triplet state with a d-vector along the z-direction, whose in-plane spin susceptibility is not expected to change as the superconducting state sets in. Based on this fact, order parameters in the blue sectors (iv), (v) and (vi), which include the originally proposed chiral p-wave state, seem not to be good candidates. Considering now the evidence for line nodes from specific heat[21–25], ultrasound attenuation[26] and recent thermal transport[27], gap structures without symmetry protected nodes in the (i) and (ix) sectors do not seem to satisfy the constraints imposed by the observations. Furthermore, muon spin rotation[15,16] and polar Kerr effect[17] experiments observe the onset of time-reversal symmetry breaking, and ultrasound measurements[26] observe a drop in the shear modulus below the critical temperature. These two observations, from experiments of very different nature, in principle require an order parameter belonging to a two-dimensional Irrep[33].

After these considerations, the order parameters which are in accordance with the observed phenomenology belong to sectors (iii), (vii) or ($viii$). Note that these always carry horizontal line nodes (some also with vertical line nodes). We can now write explicitly the form of the intra-orbital components of the best candidate order parameters. Starting with the singlet states in sector (iii),

we have a TRSB state with horizontal line nodes:

$$\Delta_{SRO}^S(\mathbf{k}) = \sum_a (d_a^{xz}(\mathbf{k}) + \alpha d_a^{yz}(\mathbf{k})) \lambda_a \otimes \sigma_0(i\sigma_2), \quad (9)$$

where $a = \{0, 7, 8\}$, α is a complex coefficient and the functions $d_a^X(\mathbf{k})$ transform as X under the point group operations. For the triplet states in sectors (vii) or ($viii$), we write TRSB triplet states with in-plane d-vector and horizontal and possibly also vertical line nodes:

$$\Delta_{SRO}^T(\mathbf{k}) = \sum_a d_a^X(\mathbf{k}) \left(\lambda_a \otimes \sigma_1 + \alpha \lambda_a \otimes \sigma_2 \right) (i\sigma_2) \quad (10)$$

where $X = \{A_1, A_2, B_1, B_2\}$.

IV. SUPERCONDUCTING FITNESS ANALYSIS

The concept of superconducting fitness proved itself useful for the understanding of the effects of external symmetry breaking fields in complex multi-orbital superconductors, and also gives a measure of the intrinsic robustness of different superconducting states within a given normal state electronic structure[31,32,34]. The superconducting fitness functions are defined as[31,32]:

$$F_C(\mathbf{k}) = H_0(\mathbf{k})\Delta(\mathbf{k}) - \Delta(\mathbf{k})H_0^*(-\mathbf{k}), \quad (11)$$
$$F_A(\mathbf{k}) = H_0(\mathbf{k})\Delta(\mathbf{k}) + \Delta(\mathbf{k})H_0^*(-\mathbf{k}).$$

Note that these are in fact matrices, which take into account the normal state electronic structure in $H_0(\mathbf{k})$ and the superconducting gap in $\Delta(\mathbf{k})$, both encoding as many microscopic degrees of freedom as needed. The averages over the Fermi surface of $Tr[|F_A(\mathbf{k})|^2]$ and $Tr[|F_C(\mathbf{k})|^2]$ were shown to directly determine the critical temperature for two-orbital scenarios[32]. The larger $F_A(\mathbf{k})$, the higher the critical temperature, while a finite $F_C(\mathbf{k})$ introduces detrimental effects to the superconducting state, reducing the critical temperature.

We apply this framework to Sr_2RuO_4, and the results for $F_A(\mathbf{k})$ and $F_C(\mathbf{k})$ are summarized in Table V and VI, respectively. We highlight that, among the intra-orbital order parameters, the terms which contribute to a finite $F_C(\mathbf{k})$ in the standard two-dimensional model are: $(1, 0)$, associated with inter-orbital hopping, carrying a form factor in B_2 (even); and $(4, 3)$ and $(5, 2) - (6, 1)$ in A_1 (even), associated with atomic SOC. In order to reduce the detrimental effects introduced by a finite $F_C(\mathbf{k})$ function, we would like to combine these terms with order parameters with non-trivial form factors $d_{ab}(\mathbf{k})$, preferably with nodal basis functions orthogonal to B_2 (even), for both singlet and triplet states. Analysing now $F_A(\mathbf{k})$, we focus on the largest contributions to the normal state Hamiltonian, given by the intra-orbital hopping terms $(7, 0)$ in B_1 (even) and $(8, 0)$ in A_1 (even). In order to maximize the average of $Tr[|F_A(\mathbf{k})|^2]$ over the Fermi surface for the singlet states, order parameters with $d_{ab}(\mathbf{k})$ in A_1 (even) would be preferred, but under the condition that these should be nodal in order to minimize $Tr[|F_C(\mathbf{k})|^2]$, the best form factor would be in the

$Tr[\|F_A(\mathbf{k})\|^2]$	2D					3D	
$[a,b]$	(1,0)	(7,0)	(8,0)	a-SOC	2D-deg	IOH-z	k-SOC
$[0,0]$	1	1	1	3		2	4
$[7,0]$	-	3/2	1/2	3/4		3/4	3/4
$[8,0]$	1/2	1/2	3/2	3/4		1/4	5/4
$[0,3]$	1	1	1	1	*	2	2
$[7,3]$	-	3/2	1/2	3/4	(**)	3/4	15/4
$[8,3]$	1/2	1/2	3/2	11/4	(***)	1/4	1/4
$\{[0,1],[0,2]\}$	1	1	1	1	*	2	1
$\{[7,1],[7,2]\}$	-	3/2	1/2	9/4	(**)	3/4	9/4
$\{[8,1],[8,2]\}$	1/2	1/2	3/2	5/4	(***)	1/4	11/4

$Tr[\|F_C(\mathbf{k})\|^2]$	2D					3D	
$[a,b]$	(1,0)	(7,0)	(8,0)	a-SOC	2D-deg	IOH-z	k-SOC
$[0,0]$	-	-	-	-		-	-
$[7,0]$	3/2	-	-	9/4		3/4	15/4
$[8,0]$	-	-	-	9/4		9/4	9/4
$[0,3]$	-	-	-	2	*	-	2
$[7,3]$	3/2	-	-	9/4	(**)	3/4	3/4
$[8,3]$	-	-	-	1/4	(***)	9/4	13/4
$\{[0,1],[0,2]\}$	-	-	-	2	*	-	3
$\{[7,1],[7,2]\}$	3/2	-	-	9/4	(**)	3/4	9/4
$\{[8,1],[8,2]\}$	-	-	-	7/4	(***)	9/4	3/4

TABLE V. Superconducting Fitness analysis for different matrix basis $[a,b]$ of $\Delta(\mathbf{k})$ indicated in the first column. The table displays the contribution of each term (c,d) in $H_0(\mathbf{k})$ for the superconducting fitness parameters as $Tr[\|F_A(\mathbf{k})\|^2] = \frac{64}{9}\sum_{cd}(\text{table entry})|d_{ab}(\mathbf{k})|^2|h_{cd}(\mathbf{k})|^2$. Columns 2-5 include terms present in a two dimensional effective model, while columns 7-8 introduce additional terms allowed in a three dimensional model. Here a-SOC stands for atomic SOC, associated with terms $(4,3)$ and $(5,2)-(6,1)$; IOH-z stands for inter-orbital inter-plane hopping associated with $\{(3,0),-(2,0)\}$, k-SOC is associated with momentum-dependent SOC from $\{(4,2),-(4,1)\}$ and $\{(5,3),(6,3)\}$. The column labelled 2D-deg indicates by asterisks which pairs of order parameters are degenerate for a two dimensional model (quasi-degeneracies are indicated by asterisks in parenthesis). Note that for a three dimensional model no degeneracies are left.

TABLE VI. Superconducting Fitness analysis. Contributions for the quantity $Tr[\|F_C(\mathbf{k})\|^2]$. Same notation as Table V.

$B_1 \sim (k_x^2 - k_y^2)$ (even) channel. For triplet states, to maximize $Tr[\|F_A(\mathbf{k})\|^2]$, a form factor in $B_2 \sim (k_x^2 - k_y^2)k_z$ (odd) is the most favoured. Concerning the choice of singlet versus triplet states, the superconducting fitness analysis finds singlet states to be the most robust, what is guaranteed by atomic SOC, as can be inferred by the larger coefficient for a-SOC in the first line of Table V.

A. Order parameter degeneracy

From Table V we can also review the discussion about the accidental degeneracies of the order parameters. We start considering a two dimensional model. It is usually stated that the helical and chiral order parameters are degenerate up to the inclusion of SOC. This argument can be based on a phenomenological Ginzburg-Landau theory, with SOC being introduced at the free energy level by evaluating the expectation value of $\boldsymbol{L}\cdot\boldsymbol{S}$ for a given pair wave-function[35,36], or from the analysis of its effects on different pairing mechanisms[37–39]. Here we analyze the degeneracy directly from a microscopic perspective, considering an orbital and spin symmetric

microscopic interaction. According to the concept of superconducting fitness[32], in the weak coupling limit, the critical temperature depends only on the averages over the Fermi surface of the superconducting fitness parameters. In the context of two dimensional models, we find that the order parameters marked with one asterisk in Tables V and VI have exactly the same $F_A(\mathbf{k})$ and $F_C(\mathbf{k})$ (assuming the same form factors $d_{ab}(\mathbf{k})$). This means that these order parameters are in fact degenerate and would have the same critical temperature within a single band scenario (or with three equivalent bands). This perspective tells us that atomic SOC does not split the degeneracy between different d-vector directions, and suggests that a rotation of the d-vector in presence of magnetic field is possible. In addition, we would like to highlight that the contributions of inter-orbital hopping $\sim 0.01t$ and SOC $\sim 0.1t$ introduce shifts of $10^{-2}-10^{-4}$ to $Tr[\|F_A(\mathbf{k})\|^2]$, taking as baseline intra-orbital hopping terms (here t stands for the maximal intra-layer intra-orbital hopping amplitude[30]). If we neglect these shifts, we have quasi-degeneracies which are not protected by symmetry, therefore not usually discussed (marked by asterisks between parenthesis in Tables V and VI). This fact is related to the almost degenerate superconducting states recently found in numerical approaches[30]. There is also an apparent unexpected degeneracy between singlet and triplet order parameters $[3,0]$ and $[3,3]$. A degeneracy would assume the same form factor $d_{ab}(\mathbf{k})$, what is not possible given the different parity of the order parameter in both cases.

B. Order parameters coupling to the lattice

It is interesting now to consider some consequences of these symmetry considerations and quasi-degeneracies for the interpretation of experiments under uniaxial

strain $\sim \epsilon_{xx} - \epsilon_{yy}$, in which case the point group is reduced from D_4 to D_2[29]. Given that inversion and time-reversal symmetries are preserved, there are no new (a,b) terms allowed in $H_0(\mathbf{k})$, and the matrix basis $[a,b]$ for the order parameters can be separated in even and odd momenta as before. As D_4 is reduced to D_2, we can make the following correspondence of Irreps: A_1 and $B_1 \rightarrow A$, A_2 and $B_2 \rightarrow B_1$ and $E \rightarrow \{B_2, B_3\}$. The last correspondence means that the two-dimensional representation E of D_4 splits into two one-dimensional representations of D_2, B_2 and B_3, under strain.

If we consider the degenerate (and quasi-degenerate) basis matrixes suggested by the superconducting fitness analysis, marked with asterisks in Tables V and VI, we find that these indicate a (quasi-)degeneracy of order parameters with a d-vector in-plane and along the z-direction for any type of intra-orbital pairing. Consulting Table III assuming the same form factor $d_{ab}(\mathbf{k})$ for both order parameters, we find that this implies a (quasi-)degeneracy of order parameters in a one-dimensional representation and in the two-dimensional representation E. Under strain, these would necessarily map into different Irreps of D_2, corresponding to the splitting of the superconducting transition.

Interestingly, the mapping of Irreps from D_4 to D_2 suggests a peculiar possibility: if there are quasi-degenerate order parameters in the A_i and B_i representations, $i = \{1, 2\}$, the introduction of strain would not lead to a splitting of the superconducting transition since in D_2 these belong to the same Irrep. Going beyond the quasi-degeneracies suggested by the superconducting fitness analysis, we can look at more exotic cases of accidental degeneracies. For example, consulting Table III, if we choose a form factor $d_{ab}(\mathbf{k})$ in B_2, its composition with basis matrixes $[0, 3]$ or $[8, 3]$ in A_2, would generate an order parameter in the B_1 representation, while its composition with the basis matrix $[7, 3]$ in B_2 would generate an order parameter in the A_1 representation. Note that all these basis matrices correspond to intra-orbital pairing and d-vector along the z-direction, with the difference that $[0, 3]$ and $[8, 3]$ introduce intra-orbital order parameters for orbitals xz and yz with same amplitude and phase, while $[7, 3]$ introduces intra-orbital order parameters for orbitals xz and yz with same amplitude but opposite phase. Note that if the magnitude of the order parameters for these two orbitals is not the same, the order parameter should necessarily include basis matrices $[a, 3]$ $(a = 0, 8)$ and $[7, 3]$, and as a consequence the order paramater would have components both in the B_1 and A_1 representations. Note that this is in agreement with the mapping of the Irreps from D_4 to D_2. This scenario is likely to happen around defects and interfaces, where the two orbitals become inequivalent. Given this example, we summarize in Table VII the different types of quasi-degeneracies and their consequences for experiments under strain.

Another interesting experiment which allows us to infer about the symmetry of the order parameter as it

Accidental degeneracy	Product	Under strain	Couples to c_{66}
A_1 and A_2	A_2	Split	No
A_1 and B_1	B_1	No Split	No
A_1 and B_2	B_2	Split	Yes
A_2 and B_1	B_2	Split	Yes
A_2 and B_2	B_1	No Split	No
B_1 and B_2	A_2	Split	No
$\{A_1, A_2, B_1, B_2\}$ and E	E	Split	Yes

TABLE VII. Summary of the experimental consequences of accidental degeneracies under strain, indicating if these split or do not split, as well as if the respective combination of order parameters would allow for coupling to the c_{66} mode in ultrasound attenuation experiments.

couples to the lattice is ultrasound attenuation. Experiments have observed a sharp decrease of the transverse sound velocity, related to the elastic constant c_{66}, in B_2, across the critical temperature[26]. The coupling of the order parameter to a lattice mode with B_2 symmetry is in principle expected only if the order parameter is in the two-dimensional representation E[33]. As a more unusual possibility, we can consider the accidental degeneracies discussed above in order to check in which cases a coupling to c_{66} is allowed. The results are summarized in Table VII. If there is an accidental degeneracy between A_1 and B_2, or between A_2 and B_1 such coupling would be possible. Note, though, that there is no accidental degeneracy that would not lead to a splitting of the critical temperature under uniaxial strain and at the same time would lead to coupling to the mentioned transverse lattice mode. This result might indicate that further microscopic work concerning the coupling of different order parameters to the lattice might be required in order to understand if there are new selection rules that emerge due to the multi-orbital nature of the order parameter.

C. Time-reversal symmetry

Time-reversal symmetry breaking has been observed below T_c by muon spin rotation[15,16] and polar Kerr effect measurements[17]. TRSB is associated with multicomponent order parameters, and in the case of Sr_2RuO_4 it has been specially related to the chiral p-wave state in the E representation. Given that the standard chiral p-wave state does not seem to account for several other experimental observations, we now need to consider other two-dimensional order parameters in order to understand this phenomen. As discussed in Section III B, good candidates are the singlet chiral d-wave state, or triplet two dimensional representations with in-plane d-vector. Another possibility is the composition of two quasi-degenerate order parameters as discussed in the

previous section, what would fit well with the absence of splitting at the transition for certain combinations of Irreps. Recent works have proposed that a singlet order parameter of the type $s + id_{x^2-y^2}$[40] would also be a possibility. This type of superposition is beyond what we can infer based on the symmetry analysis of our study.

V. DISCUSSION AND CONCLUSION

From the extended classification of the order parameters for Sr_2RuO_4 in the orbital basis, we find that the best spin singlet candidate order parameter is given by Eq. 9 with $d_{ab}(\mathbf{k})$ in $E \sim \{k_x k_z, k_y k_z\}$, while the best triplet order parameter is the one in Eq. 10 with $d_{ab}(\mathbf{k})$ in $B_2 \sim (k_x^2 - k_y^2)k_z$. Given the k_z dependence of these order parameters, it is now important to carefully consider inter-layer couplings, within a full three dimensional model. Recent works highlight the non-trivial effects of the third dimension in Sr_2RuO_4, within which one can identify a non-trivial texture in the spin and orbital DOF along the Fermi surface[41–43]. Previous theoretical proposals already have suggested order parameters which are odd along the z-direction[44–47], and therefore should be closely revisited.

As a first step in this direction, we have evaluated the superconducting fitness functions including the out-of-plane terms in the normal state Hamiltonian which are usually neglected. One interesting finding is that, within the assumption of a spin- and orbital-independent interaction, only the inter-layer terms introduce a splitting between triplet states with d-vector along the z-direction or in-plane. Note that this effect is expected to be smaller than the one previously discussed splitting of the triplet order parameters based on the value of the atomic SOC.

Richer possibilities can emerge when we consider the contribution of inter-orbital pairing[48,49]. As can be inferred from the tables in Appendix C, there is a series of inter-orbital order parameters which fall in one of the five Irreps of the point group, and will therefore coexist with intra-orbital components discussed here. A similar analysis of the superconducting fitness functions can indicate which basis matrices are degenerate for a given Irrep of the form factors $d_{ab}(\mathbf{k})$. A construction of a detailed Ginzburg-Landau functional from a microscopic perspective could elucidate what is the most suitable superposition of these different basis matrices. This is an important direction for future work in order to better understand the nature of the order parameter in Sr_2RuO_4, and how the different building blocks of the order parameter couple to external fields.

In conclusion, we analysed Sr_2RuO_4 from a microscopic perspective, with the most general single-particle Hamiltonian describing the normal state based on the orbitals in the t_{2g} manifold and reclassifying the order parameters in the orbital basis. These constructions use the point group symmetry and on the orbital character of the underlying DOFs. We propose new order parameter candidates which allow for the consistent understanding of many experimental results available at the moment. From the observed phenomenology, the best candidate order parameters are: a singlet state or a triplet superconductor with an in-plane d-vector. From the superconducting fitness analysis, we determine that the most robust order parameter is a trivial singlet state with form factors in the B_1 representation. Among the triplet states, an order parameter with a form factor in the B_2 representation is the most robust, what would imply the presence of both horizontal and vertical line nodes. Furthermore, we find that for a two-dimensional model with orbital and spin symmetric interactions, the order parameter with in plane d-vector is in fact degenerate with the triplet state with d-vector along the z-direction even in presence of atomic SOC. Interestingly, this degeneracy is lifted only by inter-layer processes. Extra quasi-degeneracies can also be identified, and could be associated with unusual types of order parameter superpositions. Our work does not concern the pairing mechanism, but provides a detailed classification of the order parameters from the orbital perspective and probe these against the available experimental results and within the concept of superconducting fitness. Our analysis should motivate a reconsideration of theories which take into account the role of inter-layer processes and the construction of interacting models from an orbital perspective, considering the role of Hund's coupling[50,51], in order to elucidate the origin of superconductivity in Sr_2RuO_4 from a microscopic perspective.

Appendix A: Gell-Mann Matrices and Pauli Matrices

The Gell-Mann matrices used in this work are the following:

$$\lambda_1 = \begin{pmatrix} 0 & 1 & 0 \\ 1 & 0 & 0 \\ 0 & 0 & 0 \end{pmatrix}, \qquad \lambda_2 = \begin{pmatrix} 0 & 0 & 1 \\ 0 & 0 & 0 \\ 1 & 0 & 0 \end{pmatrix}, \qquad (A1)$$

$$\lambda_3 = \begin{pmatrix} 0 & 0 & 0 \\ 0 & 0 & 1 \\ 0 & 1 & 0 \end{pmatrix}, \qquad \lambda_4 = \begin{pmatrix} 0 & -i & 0 \\ i & 0 & 0 \\ 0 & 0 & 0 \end{pmatrix},$$

$$\lambda_5 = \begin{pmatrix} 0 & 0 & -i \\ 0 & 0 & 0 \\ i & 0 & 0 \end{pmatrix}, \qquad \lambda_6 = \begin{pmatrix} 0 & 0 & 0 \\ 0 & 0 & -i \\ 0 & i & 0 \end{pmatrix},$$

$$\lambda_7 = \begin{pmatrix} 1 & 0 & 0 \\ 0 & -1 & 0 \\ 0 & 0 & 0 \end{pmatrix}, \qquad \lambda_8 = \frac{1}{\sqrt{3}}\begin{pmatrix} 1 & 0 & 0 \\ 0 & 1 & 0 \\ 0 & 0 & -2 \end{pmatrix}.$$

We also define

$$\lambda_0 = \sqrt{\frac{2}{3}}\begin{pmatrix} 1 & 0 & 0 \\ 0 & 1 & 0 \\ 0 & 0 & 1 \end{pmatrix}. \qquad (A2)$$

Note that all matrices follow $Tr[\lambda_j^2] = 2$.
The Pauli matrices used are the following:

$$\sigma_1 = \begin{pmatrix} 0 & 1 \\ 1 & 0 \end{pmatrix}, \quad \sigma_2 = \begin{pmatrix} 0 & -i \\ i & 0 \end{pmatrix}, \quad \sigma_3 = \begin{pmatrix} 1 & 0 \\ 0 & -1 \end{pmatrix}, (A3)$$

and

$$\sigma_0 = \begin{pmatrix} 1 & 0 \\ 0 & 1 \end{pmatrix}. \qquad (A4)$$

Note that all matrices follow $Tr[\sigma_j^2] = 2$.

Appendix B: Point group D_4

As stated in the main text, Sr_2RuO_4 has the tetragonal space group $I4/mmm$, or #139. This group consists of operations in the point group D_4 (total of 8 operations), as well as its combination with inversion (totalling 16 operations). There are also another set of 16 operations which are related to intra-unit-cell shifts by half lattice constant in all directions.

Given the strong two-dimensional phenomenology of this material, Sr_2RuO_4 is usually described by a model on the square lattice, what would suggest C_4 symmetry, but here the transformations which consider rotations along in-plane axes are also important because of the odd character of some of the orbitals along the z-direction. We therefore start with D_4 symmetry, a group which has 8 elements arranged in five conjugacy classes:

- E: Identity.

- $2C_4$: two rotations along the z-axis, one by $\pi/2$ and another by $3\pi/2$.

- C_2: a rotation along the z-axis by π.

- $2C_2'$: rotations by π along the x- or y- axis.

- $2C_2''$: rotations by π along the diagonals $d(x = y)$ or $\bar{d}(x = -y)$.

Given the five conjugacy classes, there are five irreducible representations. Below we have the character table of D_4 highlighting the irreducible representations and the associated even and odd lowest order basis functions:

D_4	E	$2C_4$	C_2	$2C_2'$	$2C_2''$	Even Basis	Odd Basis
A_1	+1	+1	+1	+1	+1	1	$xyz(x^2 - y^2)$
A_2	+1	+1	+1	-1	-1	$xy(x^2 - y^2)$	z
B_1	+1	-1	+1	+1	-1	$x^2 - y^2$	xyz
B_2	+1	-1	+1	-1	+1	xy	$z(x^2 - y^2)$
E	+2	0	-2	0	0	$\{xz, yz\}$	$\{x, y\}$

Note that all the operations can be written in terms of C_4, C_{2x}', C_{2d}'':

- $E = C_4^4$,

- $C_2 = C_4^2$,

- $C_{2y}' = C_4 C_{2x}' C_4^{-1}$.

- $C_{2\bar{d}}'' = C_4 C_{2d}'' C_4^{-1}$,

so if the system is invariant under C_4, C_{2x}', C_{2d}'', it is invariant under all transformations of the point group. One can think of these operations as the generators of the group. Note that we should consider also inversion P to complete the point group D_{4h} associated with I4/mmm.

1. Generators acting on coordinates

The generators identified above act on the spatial coordinates as follows:

$$C_4 = \begin{cases} x \to y \\ y \to -x \\ z \to z \end{cases}, \qquad C_{2x}' = \begin{cases} x \to x \\ y \to -y \\ z \to -z \end{cases}, \quad (B1)$$

$$C''_{2d} = \begin{cases} x \to y \\ y \to x \\ z \to -z \end{cases} , \qquad P = \begin{cases} x \to -x \\ y \to -y \\ z \to -z \end{cases} .$$

2. Generators acting on orbitals

Considering the orbitals in the t_{2g} manifold in the basis $\Phi^\dagger = (c^\dagger_{yz}, c^\dagger_{xz}, c^\dagger_{xy})$, the basic operations above can be written as:

$$C_4 = \begin{pmatrix} 0 & 1 & 0 \\ -1 & 0 & 0 \\ 0 & 0 & -1 \end{pmatrix}, \qquad (B2)$$

$$C'_{2x} = \begin{pmatrix} 1 & 0 & 0 \\ 0 & -1 & 0 \\ 0 & 0 & -1 \end{pmatrix},$$

$$C''_{2d} = \begin{pmatrix} 0 & -1 & 0 \\ -1 & 0 & 0 \\ 0 & 0 & 1 \end{pmatrix},$$

$$P = \begin{pmatrix} 1 & 0 & 0 \\ 0 & 1 & 0 \\ 0 & 0 & 1 \end{pmatrix}.$$

3. Generators acting on spin

Considering the spin DOF in the basis $\Phi^\dagger = (c^\dagger_\uparrow, c^\dagger_\downarrow)$, the basic operations above can be written as:

$$C_4 = \frac{\sigma_0 - i\sigma_3}{\sqrt{2}}, \qquad (B3)$$

$$C'_{2x} = i\sigma_1,$$

$$C''_{2d} = i\frac{(\sigma_1 + \sigma_2)}{\sqrt{2}},$$

$$P = \sigma_0.$$

Appendix C: Irreducible representations of the matrix-basis of the order parameters

Here we summarize the properties of the 15 matrices which would pair with even $d_{ab}(\mathbf{k})$ functions:

$[a,b]$	Irrep	Orbital	Spin
$[0,0]$	A_1	Intra	Singlet
$[4,3]$	A_1	Singlet	Triplet
$[8,0]$	A_1	Intra	Singlet
$[5,2] - [6,1]$	A_1	Singlet	Triplet
$[5,1] + [6,2]$	A_2	Singlet	Triplet
$[7,0]$	B_1	Intra	Singlet
$[5,2] + [6,1]$	B_1	Singlet	Triplet
$[1,0]$	B_2	Triplet	Singlet
$[5,1] - [6,2]$	B_2	Singlet	Triplet
$[3,0]$	$E(i)$	Triplet	Singlet
$-[2,0]$	$E(i)$	Triplet	Singlet
$[4,2]$	$E(ii)$	Singlet	Triplet
$-[4,1]$	$E(ii)$	Singlet	Triplet
$[5,3]$	$E(iii)$	Singlet	Triplet
$[6,3]$	$E(iii)$	Singlet	Triplet

Here we summarize the properties of the 21 matrices   .
which would pair with odd $d_{ab}(\mathbf{k})$ functions:

$[a, b]$	Irrep	Orbital	Spin
$[2,2] - [3,1]$	A_1	Triplet	Triplet
$[0,3]$	A_2	Intra	Triplet
$[4,0]$	A_2	Singlet	Singlet
$[8,3]$	A_2	Intra	Triplet
$[7,3]$	B_2	Intra	Triplet
$[2,1] + [3,2]$	A_2	Triplet	Triplet
$[1,3]$	B_1	Intra	Triplet
$[2,2] + [3,1]$	B_1	Triplet	Triplet
$[2,1] - [3,2]$	B_2	Triplet	Triplet
$[0,1]$	$E(i)$	Intra	Triplet
$[0,2]$	$E(i)$	Intra	Triplet
$[1,2]$	$E(ii)$	Triplet	Triplet
$[1,1]$	$E(ii)$	Triplet	Triplet
$[2,3]$	$E(iii)$	Triplet	Triplet
$[3,3]$	$E(iii)$	Triplet	Triplet
$[6,0]$	$E(iv)$	Singlet	Singlet
$-[5,0]$	$E(iv)$	Singlet	Singlet
$[7,1]$	$E(v)$	Intra	Triplet
$-[7,2]$	$E(v)$	Intra	Triplet
$[8,1]$	$E(vi)$	Intra	Triplet
$[8,2]$	$E(vi)$	Intra	Triplet

[1] A. P. Mackenzie and Y. Maeno, Rev. Mod. Phys. **75**, 657 (2003).

[2] Z. Mao, Y. Maeno, and H. Fukazawa, Materials Research Bulletin **35**, 1813 (2000).

[3] A. P. Mackenzie, S. R. Julian, A. J. Diver, G. J. McMullan, M. P. Ray, G. G. Lonzarich, Y. Maeno, S. Nishizaki, and T. Fujita, Phys. Rev. Lett. **76**, 3786 (1996).

[4] C. Bergemann, S. R. Julian, A. P. Mackenzie, S. Nishizaki, and Y. Maeno, Phys. Rev. Lett. **84**, 2662 (2000).

[5] Y. Maeno, K. Yoshida, H. Hashimoto, S. Nishizaki, S.-i. Ikeda, M. Nohara, T. Fujita, A. Mackenzie, N. Hussey, J. Bednorz, and F. Lichtenberg, Journal of the Physical Society of Japan **66**, 1405 (1997), https://doi.org/10.1143/JPSJ.66.1405.

[6] A. Damascelli, D. H. Lu, K. M. Shen, N. P. Armitage, F. Ronning, D. L. Feng, C. Kim, Z.-X. Shen, T. Kimura, Y. Tokura, Z. Q. Mao, and Y. Maeno, Phys. Rev. Lett. **85**, 5194 (2000).

[7] A. P. Mackenzie, T. Scaffidi, C. W. Hicks, and Y. Maeno, npj Quantum Materials **2**, 40 (2017).

[8] T. Nomura and K. Yamada, Journal of the Physical Society of Japan **69**, 3678 (2000), https://doi.org/10.1143/JPSJ.69.3678.

[9] T. Nomura and K. Yamada, Journal of the Physical Society of Japan **71**, 1993 (2002), https://doi.org/10.1143/JPSJ.71.1993.

[10] K. Miyake and O. Narikiyo, Phys. Rev. Lett. **83**, 1423 (1999).

[11] T. Kuwabara and M. Ogata, Phys. Rev. Lett. **85**, 4586 (2000).

[12] K. Ishida, H. Mukuda, Y. Kitaoka, K. Asayama, Z. Q. Mao, Y. Mori, and Y. Maeno, Nature **396**, 658 EP (1998).

[13] K. Ishida, M. Manago, T. Yamanaka, H. Fukazawa, Z. Q. Mao, Y. Maeno, and K. Miyake, Phys. Rev. B **92**, 100502(R) (2015).

[14] J. A. Duffy, S. M. Hayden, Y. Maeno, Z. Mao, J. Kulda, and G. J. McIntyre, Phys. Rev. Lett. **85**, 5412 (2000).

[15] G. M. Luke, Y. Fudamoto, K. M. Kojima, M. I. Larkin, J. Merrin, B. Nachumi, Y. J. Uemura, Y. Maeno, Z. Q. Mao, Y. Mori, H. Nakamura, and M. Sigrist, Nature **394**, 558 EP (1998).

[16] G. Luke, Y. Fudamoto, K. Kojima, M. Larkin, B. Nachumi, Y. Uemura, J. Sonier, Y. Maeno, Z. Mao, Y. Mori, and D. Agterberg, Physica B: Condensed Matter **289-290**, 373 (2000).

[17] J. Xia, Y. Maeno, P. T. Beyersdorf, M. M. Fejer, and A. Kapitulnik, Phys. Rev. Lett. **97**, 167002 (2006).

[18] T. M. Rice and M. Sigrist, Journal of Physics: Condensed Matter **7**, L643 (1995).

[19] Y. Maeno, S. Kittaka, T. Nomura, S. Yonezawa, and K. Ishida, Journal of the Physical Society of Japan **81**, 011009 (2012), https://doi.org/10.1143/JPSJ.81.011009.

[20] C. Kallin, Reports on Progress in Physics **75** (2012), 10.1088/0034-4885/75/4/042501.

[21] S. NishiZaki, Y. Maeno, and Z. Mao, Journal of Low Temperature Physics **117**, 1581 (1999).

[22] S. NishiZaki, Y. Maeno, and Z. Mao, Journal of the Physical Society of Japan **69**, 572 (2000), https://doi.org/10.1143/JPSJ.69.572.

[23] K. Deguchi, Z. Q. Mao, H. Yaguchi, and Y. Maeno, Phys. Rev. Lett. **92**, 047002 (2004).

[24] K. Deguchi, Z. Q. Mao, and Y. Maeno, Journal of the Physical Society of Japan **73**, 1313 (2004), https://doi.org/10.1143/JPSJ.73.1313.

[25] S. Kittaka, S. Nakamura, T. Sakakibara, N. Kikugawa, T. Terashima, S. Uji, D. A. Sokolov, A. P. Mackenzie, K. Irie, Y. Tsutsumi, K. Suzuki, and K. Machida, Journal of the Physical Society of Japan **87**, 093703 (2018).

[26] C. Lupien, W. A. MacFarlane, C. Proust, L. Taillefer, Z. Q. Mao, and Y. Maeno, Phys. Rev. Lett. **86**, 5986 (2001).

[27] E. Hassinger, P. Bourgeois-Hope, H. Taniguchi, S. René de Cotret, G. Grissonnanche, M. S. Anwar, Y. Maeno, N. Doiron-Leyraud, and L. Taillefer, Phys. Rev. X **7**, 011032 (2017).

[28] A. Pustogow, Y. Luo, A. Chronister, Y. S. Su, D. A. Sokolov, F. Jerzembeck, A. P. Mackenzie, C. W. Hicks, N. Kikugawa, S. Raghu, E. D. Bauer, and S. E. Brown, arXiv e-prints , arXiv:1904.00047 (2019), arXiv:1904.00047 [cond-mat.supr-con].

[29] C. A. Watson, A. S. Gibbs, A. P. Mackenzie, C. W. Hicks, and K. A. Moler, Phys. Rev. B **98**, 094521 (2018).

[30] T. Scaffidi, J. C. Romers, and S. H. Simon, Phys. Rev. B **89**, 220510(R) (2014).

[31] A. Ramires and M. Sigrist, Phys. Rev. B **94**, 104501 (2016).

[32] A. Ramires, D. F. Agterberg, and M. Sigrist, Phys. Rev. B **98**, 024501 (2018).

[33] M. Sigrist and K. Ueda, Rev. Mod. Phys. **63**, 239 (1991).

[34] A. Ramires and M. Sigrist, Journal of Physics: Conference Series **807**, 052011 (2017).

[35] M. Sigrist and M. E. Zhitomirsky, Journal of the Physical Society of Japan **65**, 3452 (1996), https://doi.org/10.1143/JPSJ.65.3452.

[36] M. Sigrist, Progress of Theoretical Physics Supplement **160**, 1 (2005), http://oup.prod.sis.lan/ptps/article-pdf/doi/10.1143/PTPS.160.1/5161961/160-1.pdf.

[37] Y. Yanase and M. Ogata, Journal of the Physical Society of Japan **72**, 673 (2003), https://doi.org/10.1143/JPSJ.72.673.

[38] J. F. Annett, G. Litak, B. L. Györffy, and K. I. Wysokiński, Phys. Rev. B **73**, 134501 (2006).

[39] K. K. Ng and M. Sigrist, Europhysics Letters (EPL) **49**, 473 (2000).

[40] A. T. Rømer, D. D. Scherer, I. M. Eremin, P. J. Hirschfeld, and B. M. Andersen, arXiv e-prints , arXiv:1905.04782 (2019), arXiv:1905.04782 [cond-mat.supr-con].

[41] M. W. Haverkort, I. S. Elfimov, L. H. Tjeng, G. A. Sawatzky, and A. Damascelli, Phys. Rev. Lett. **101**, 026406 (2008).

[42] C. N. Veenstra, Z.-H. Zhu, M. Raichle, B. M. Ludbrook, A. Nicolaou, B. Slomski, G. Landolt, S. Kittaka, Y. Maeno, J. H. Dil, I. S. Elfimov, M. W. Haverkort, and A. Damascelli, Phys. Rev. Lett. **112**, 127002 (2014).

[43] C. G. Fatuzzo, M. Dantz, S. Fatale, P. Olalde-Velasco, N. E. Shaik, B. Dalla Piazza, S. Toth, J. Pelliciari, R. Fittipaldi, A. Vecchione, N. Kikugawa, J. S. Brooks, H. M. Rønnow, M. Grioni, C. Rüegg, T. Schmitt, and J. Chang, Phys. Rev. B **91**, 155104 (2015).

[44] M. E. Zhitomirsky and T. M. Rice, Phys. Rev. Lett. **87**, 057001 (2001).

[45] J. F. Annett, G. Litak, B. L. Györffy, and K. I. Wysokiński, Phys. Rev. B **66**, 134514 (2002).

[46] W. Huang and H. Yao, Phys. Rev. Lett. **121**, 157002

(2018).

[47] H. S. Røising, F. Flicker, T. Scaffidi, and S. H. Simon, Phys. Rev. B **98**, 224515 (2018).

[48] W. Huang, Y. Zhou, and H. Yao, arXiv e-prints , arXiv:1905.03523 (2019), arXiv:1905.03523 [cond-mat.supr-con].

[49] O. Gingras, R. Nourafkan, A.-M. S. Tremblay, and M. Côté, arXiv e-prints , arXiv:1808.02527 (2018), arXiv:1808.02527 [cond-mat.supr-con].

[50] M. Cuoco, C. Noce, and A. Romano, Phys. Rev. B **57**, 11989 (1998).

[51] H. U. R. Strand, M. Zingl, N. Wentzell, O. Parcollet, and A. Georges, arXiv e-prints , arXiv:1904.07324 (2019), arXiv:1904.07324 [cond-mat.str-el].